

A comparison of atomic force microscope friction and phase imaging for the characterization of an immiscible polystyrene/poly(methyl methacrylate) blend film

Matthew F. Paige*

Department of Chemistry, University of Saskatchewan, 110 Science Place, Saskatoon, SK S7N 5C9, Canada

Received 21 February 2003; received in revised form 30 June 2003; accepted 2 July 2003

Abstract

Three different forms of atomic force microscope (AFM) measurement, topography, friction force and phase imaging, have been used to investigate the surface morphology and local composition of an immiscible polystyrene (PS)/poly(methyl methacrylate) (PMMA) blend film. This sample forms discrete, micron-size domains in a continuous matrix, which is attributed to the segregation of PMMA in PS. When the samples were imaged in air, contrast in friction and phase images was caused by variations in sample topography only. When the samples were imaged under water, however, both friction and phase imaging yielded non-topographic contrast between domains. We ascribe the contrast in both of these imaging modes to preferential softening of the hydrophilic, PMMA-rich domains and to stronger tip–sample adhesive forces, highlighting the AFM's utility for probing local elastic properties and for compositional mapping of soft polymer samples. © 2003 Elsevier Ltd. All rights reserved.

Keywords: Atomic force microscope; Polymer film; Compositional mapping

1. Introduction

Atomic force microscope imaging is a well-established technique for the characterization of polymer film morphology at sub-nanometer spatial resolution [1,2]. While of great utility, determination of film surface morphology alone is rarely sufficient to describe all of the important features of a polymer system. Significant efforts have been made to develop the AFM's ability to probe local chemical and viscoelastic properties, with the ultimate goal of simultaneous morphological and compositional mapping. Some aspects of compositional identification are intrinsic to AFM operation, as the interaction forces that exist between the tip and surface contain chemical and viscoelastic information about the sample. A number of novel imaging methods that monitor and exploit these interaction forces have recently been implemented, and have been described in a number of review articles [1,3]. Two of the most promising approaches for combined morphological and compositional mapping of polymer films that are gaining

widespread use are friction force imaging and phase imaging.

Friction force imaging, also referred to as lateral force imaging, is a variation of contact mode AFM in which friction-induced torsion of the AFM cantilever is used to construct an image of the sample. Briefly, the AFM probe tip is scanned over the sample of interest while maintaining constant tip–sample contact. The cantilever is scanned perpendicular to its main axis and torsion/lateral bending of the cantilever is measured. Torsion in the cantilever reflects a complex convolution of effects, including coupling with sample topography, tip–sample adhesive forces and viscoelastic deformation of the sample [4]. A number of important investigations have used friction force imaging to differentiate between distinct chemical regions in thin films. Particularly noteworthy studies include the use of friction imaging for the characterization of phase segregated lipid domains in Langmuir Blodgett monolayers [4] and bilayers [5], and differentiation of fluorocarbon from hydrocarbon domains in mixed organic films [6]. In most friction force imaging experiments, contrast between domains can be attributed to local variations in viscoelastic surface properties. In addition to exploiting mechanical properties, specific

* Tel.: +1-306-966-4665; fax: +1-306-966-4730.

E-mail address: matthew.paige@sask.usask.ca (M.F. Paige).

chemical interactions between functional groups have also been used to generate contrast in friction force imaging. Key work in this field has been carried out Lieber et al., who made use of chemically functionalized AFM tips in conjunction with friction imaging to yield chemically-sensitive AFM measurements [7–9]. While useful, one shortcoming of friction force imaging is that the presence of water and other surface adsorbed contaminants that are present on all samples under ambient conditions can give rise to capillary forces between tip and sample that are comparable or even larger than the frictional forces of interest. While not the case for every sample, this often requires that friction imaging be done under a liquid environment.

Another variation of AFM imaging that has demonstrated promise for composition-based surface mapping is phase imaging. In this approach, the AFM is operated in intermittent contact mode; the cantilever is oscillated near to its resonance frequency and an image is constructed by ‘tapping’ the tip over the surface. There are multiple benefits to intermittent contact imaging. Tip-sample interaction forces are greatly reduced from contact mode (~ 100 nN for contact vs ~ 100 pN for non-contact [10, 11]), minimizing plastic deformation of soft materials with the tip. Additionally, intermittent contact mode enables new methods for obtaining image contrast. By monitoring the phase lag between the cantilever driving frequency and its response, one gains a sensitive probe of polymer surface properties. The phase lag is sensitive to tip–sample adhesion, viscoelasticity and compositional variations in the sample, making it an extremely versatile probe of local properties [9,12]. However, while useful for providing image contrast, the nature of the tip–sample interactions in intermittent contact mode are not thoroughly understood and interpretation of phase images in terms of physical properties of the sample can be quite complicated. Both the magnitude and the polarity (positive or negative phase) of the phase lag is strongly dependent upon the tip–sample imaging force (typically defined by the ratio of the cantilever’s engaged or setpoint oscillation amplitude to its free air amplitude), and altering this experimental parameter can lead to significant differences in the observed phase lag [1]. In general, the phase lag is related to both energy dissipation by the sample as well as the duration of tip–sample contact time [1,12], though further effort is needed to clarify many of these effects.

In this work, we have used both friction force and phase imaging to investigate a film consisting of an immiscible polystyrene (PS)/poly(methyl methacrylate) (PMMA) polymer blend. The ultimate objective is to compare and contrast the utility of phase and friction force imaging for combined morphological and compositional mapping. The polymer samples used in this study have previously been investigated using a combination of scanning transmission X-ray microscopy (STXM), X-ray photoemission spectroscopy (X-PEEM) and topographical AFM imaging [13]. Because

the films are well characterized, we have found them to be useful standard samples for comparing different AFM imaging modes. For the film compositions used in our studies (30:70 PS/PMMA (w/w)), the X-PEEM and STXM measurements carried out previously show that the films consist of discontinuous PMMA-rich domains surrounded by a continuous domain rich in PS.

2. Materials and methods

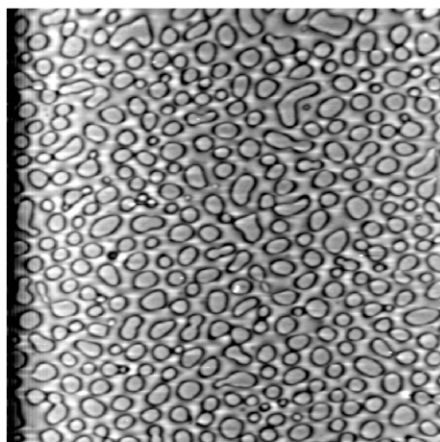
The samples used in these experiments consisted of an immiscible PS/PMMA blend film deposited by spin casting onto a silicon substrate. Samples were a generous gift from Professor A. Hitchcock, Cynthia Morin (McMaster University) and Professor Stephen Urquhart (University of Saskatchewan). The preparation of these samples is described in detail elsewhere [13]. Briefly, a 30/70 (w/w) PS/PMMA solution in toluene (total polymer by weight was 1%) was spin cast onto a silicon substrate. The polymers were purchased from Polymer Source Inc. (PS: $M_w = 1$ M; PMMA: $M_w = 310$ K). Samples were vacuum annealed for 6 h at 160°C . Control samples of the silicon substrate were featureless at the nanometer length-scale when imaged in the AFM.

AFM measurements were performed on a Molecular Imaging PicoSPM instrument (Molecular Imaging, Tempe, AZ) operating in both contact and intermittent contact (‘AC’) imaging modes. Imaging was performed both in air and under ultrapure water (Millipore), using a commercial fluid cell. For contact mode imaging, commercial ‘diving board’ shaped probe tips (MikroMasch USA, Portland, OR), with spring constants ranging from 0.3–0.8 N/m were used. Intermittent contact images were acquired using probes from the same manufacturer but with spring constants from 0.3–0.65 N/m and resonance frequencies in the range of 20–40 kHz. Unless otherwise stated, all intermittent contact measurements were taken in the ‘moderate force’ regime, with the ratio of the setpoint oscillation amplitude to free air oscillation amplitude of around 0.6–0.7. All measurements were performed with the instrument mounted in a vibration isolation system. Some topography images are shown in deflection (derivative) mode to enhance the appearance of edges; however all height measurements were taken from height mode images only.

3. Results and discussion

Typical AFM images of the polymer blend film taken using contact mode in air are shown in Fig. 1A,B. Samples consisted of a smooth, continuous domain in which numerous oblong patches, called discontinuous domains, were embedded. The discontinuous domains had a distribution of sizes, though were typically on the order of a micron in diameter. Discontinuous domains accounted for

A.



B.

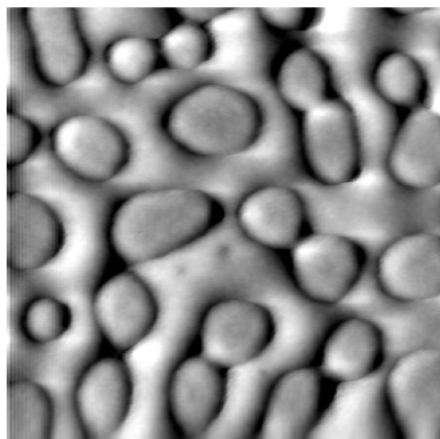


Fig. 1. A, Deflection image ($20\ \mu\text{m} \times 20\ \mu\text{m}$) of mixed PS/PMMA film on silicon using contact mode in air. B, Deflection image ($5\ \mu\text{m} \times 5\ \mu\text{m}$) of mixed PS/PMMA film on silicon using contact mode in air.

approximately 35% of the total area of the measured surface. The discontinuous domain edges were defined by a depression that fell below the plane of the continuous domain by $\sim 1\text{--}3\ \text{nm}$, while their interiors were at approximately the same elevation as the continuous domain. To verify that the tip was not damaging the sample during imaging, we repeatedly scanned a $5\ \mu\text{m} \times 5\ \mu\text{m}$ region of the sample, then imaged a $20\ \mu\text{m} \times 20\ \mu\text{m}$ area that included the previously scanned region. As seen in Fig. 2, samples treated this way showed no evidence of tip-induced damage even after multiple scans; if the sample were being damaged one would expect to see a square $5\ \mu\text{m} \times 5\ \mu\text{m}$ pattern in the center of the image. Film morphologies for these samples were slightly different from those observed previously by Morin et al. [13], who found that the discontinuous domains were elevated above the continuous domain. The exact reason for this is not clear; however, the batch of samples used in our study were annealed for approximately 4 h longer than those in Ref. [13], suggesting that small differences in sample preparation conditions can

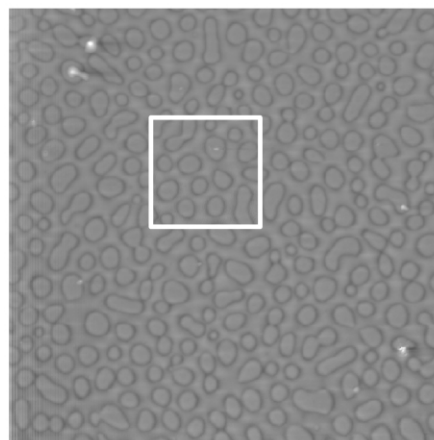


Fig. 2. Deflection image ($20\ \mu\text{m} \times 20\ \mu\text{m}$) of mixed PS/PMMA film on silicon using contact mode in air. The inset square is a $5\ \mu\text{m} \times 5\ \mu\text{m}$ region that was imaged repeatedly prior to zooming out. No tip-induced damage is visible.

lead to significantly different final surface morphologies. A more detailed study of these effects is currently underway.

From earlier X-PEEM and STXM measurements, Morin et al. [13] have found the discontinuous domains to be rich in PMMA while the continuous domains are rich in PS. In these earlier studies, samples that had not been annealed contained a large number of holes in the PMMA domains, likely caused by the formation of small PS aggregates. Annealed samples occasionally contained larger, coalesced versions of these domains, though some of the AFM data suggested that PS tended to lie below the PMMA surface. For the samples used here, we saw no evidence for the formation of PS aggregates inside the PMMA domains. As noted previously, annealing times for these samples were approximately 4 h longer than those used by Morin et al. and if the annealing process causes the PS aggregates to coalesce and diffuse below the PMMA surface, then it seems reasonable that no aggregates are visible for these samples.

In order to see if we could assess the composition of the polymer domains using the AFM in air, we collected force vs tip-sample distance curves for both the continuous and discontinuous domains. In these measurements, the tip-sample interaction force is monitored during a tip-surface approach-retract cycle. Hysteresis between the approach and retraction curves can give information about tip-sample adhesion forces which in turn depend on the chemical nature of the tip-sample interface [8]. Typical force curves (retraction) taken from a discontinuous and continuous domain are shown in Fig. 3A,B. Regardless of whether the tip was positioned on the continuous or discontinuous domain, we observed the same magnitude of tip-sample adhesion force. Measuring ten different discontinuous and continuous regions with the same tip yielded a tip-sample adhesion force of $17 \pm 3\ \text{nN}$ for the continuous domains and $15 \pm 2\ \text{nN}$ for the discontinuous domains, respectively. Note, that for these measurements,

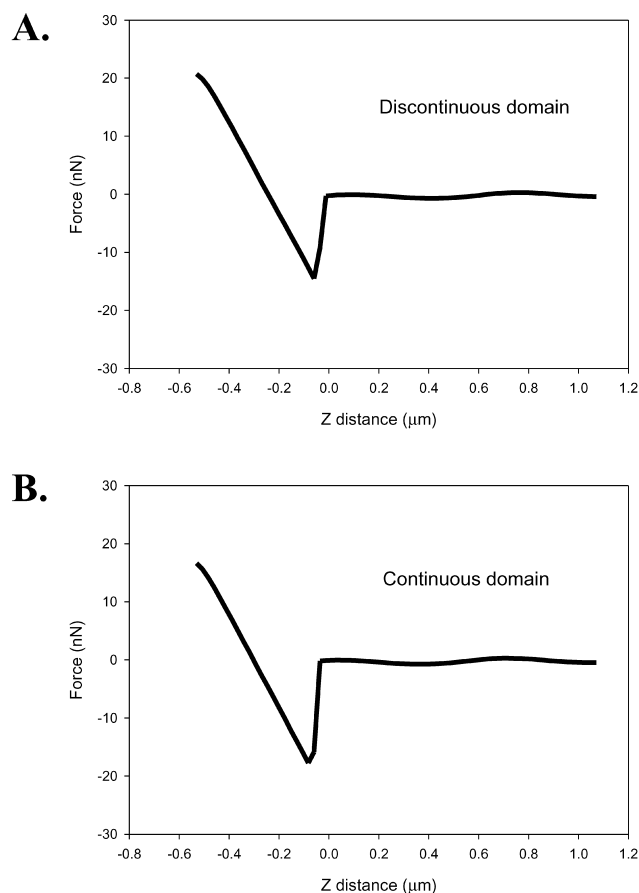


Fig. 3. A, Typical force vs distance retraction curve taken from a discontinuous domain. The mean adhesive force from $N = 10$ measurements was 17 ± 3 nN. B, Typical force vs distance retraction curve taken from a continuous domain. The mean adhesive force from $N = 10$ measurements was 15 ± 2 nN.

we assumed the manufacturer's value for the cantilever spring constant. While this may not be entirely accurate, the relative values of the measured adhesion forces will be correct since all measurements were taken with the same cantilever.

Since commercial Si_3N_4 AFM tips are slightly hydrophilic, one might reasonably expect to see stronger tip-sample adhesion with the hydrophilic PMMA-rich domains over the PS-rich domains. One might also expect that the hydrophilic PMMA-rich domains would be more thoroughly covered with water than the PS-rich domains, again leading to higher adhesive forces. However, this was simply not the case; within the error of the experiment, the measured values for adhesion force were the same for both domains. This is likely because differences in adhesion forces between the domains are very small in comparison with capillary forces induced by surface-bound water that saturates the entire polymer surface under ambient conditions. The latter effect dominates the measurement and inhibits the ability to resolve small differences in adhesive forces.

To overcome the effect of capillary forces, the samples

were imaged under ultrapure water. When imaged under water, the film retains its gross structure as shown in Fig. 4. As was the case in air, tip-sample interaction forces were sufficiently small to allow stable, reproducible imaging without tip-induced damage; multiple images of the same region could be collected without detectable change. However, unlike the images collected in air, fine structural details in the continuous domain could be resolved under water. Cross-sections taken from typical regions of the continuous and discontinuous domains, in both air and water, are shown in Fig. 5A–D. For the continuous domain in water, vertical features on the order of ~ 1 nm are resolvable. A small change in surface morphology may also exist for the discontinuous domains when immersed in water, though the surface features that are resolved under fluid appear as digitized steps (individual analog-to-digital converter elements) and are at the extreme edge of the instrument's detection limit. To further explain these effects, we again measured force vs tip-sample distance curves for the different polymer domains. For both the continuous and discontinuous domains, the tip was found to penetrate and damage the polymer surface. While the applied loading force we used for imaging experiments was not sufficiently high to cause damage, force-curve measurements typically scan a wide range of loading forces and the higher loads were sufficiently large to damage the sample. As this damage did not occur in air, the measurements suggest that both the PMMA and PS components of the blended film soften considerably upon exposure to water.

To further explore the capacity of the AFM for compositional mapping in this system, we carried out friction force imaging both in air and under water. Some typical results from these measurements are shown in Fig. 6A–D. As noted in the Introduction, torsion of the AFM cantilever, and hence the friction image, arises from a combination of sample topography, adhesive forces and elastic deformation of the sample. A simple method for deconvoluting topographical effects from adhesion and

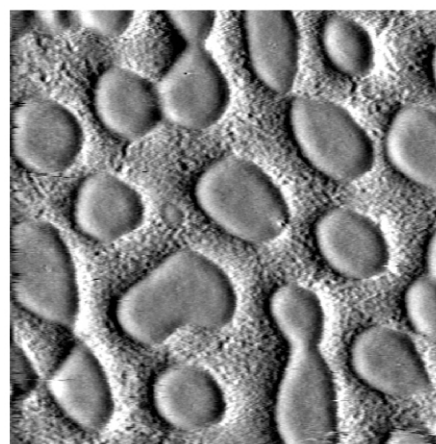


Fig. 4. Deflection image ($5 \mu\text{m} \times 5 \mu\text{m}$) of mixed PS/PMMA film on silicon using contact mode in water.

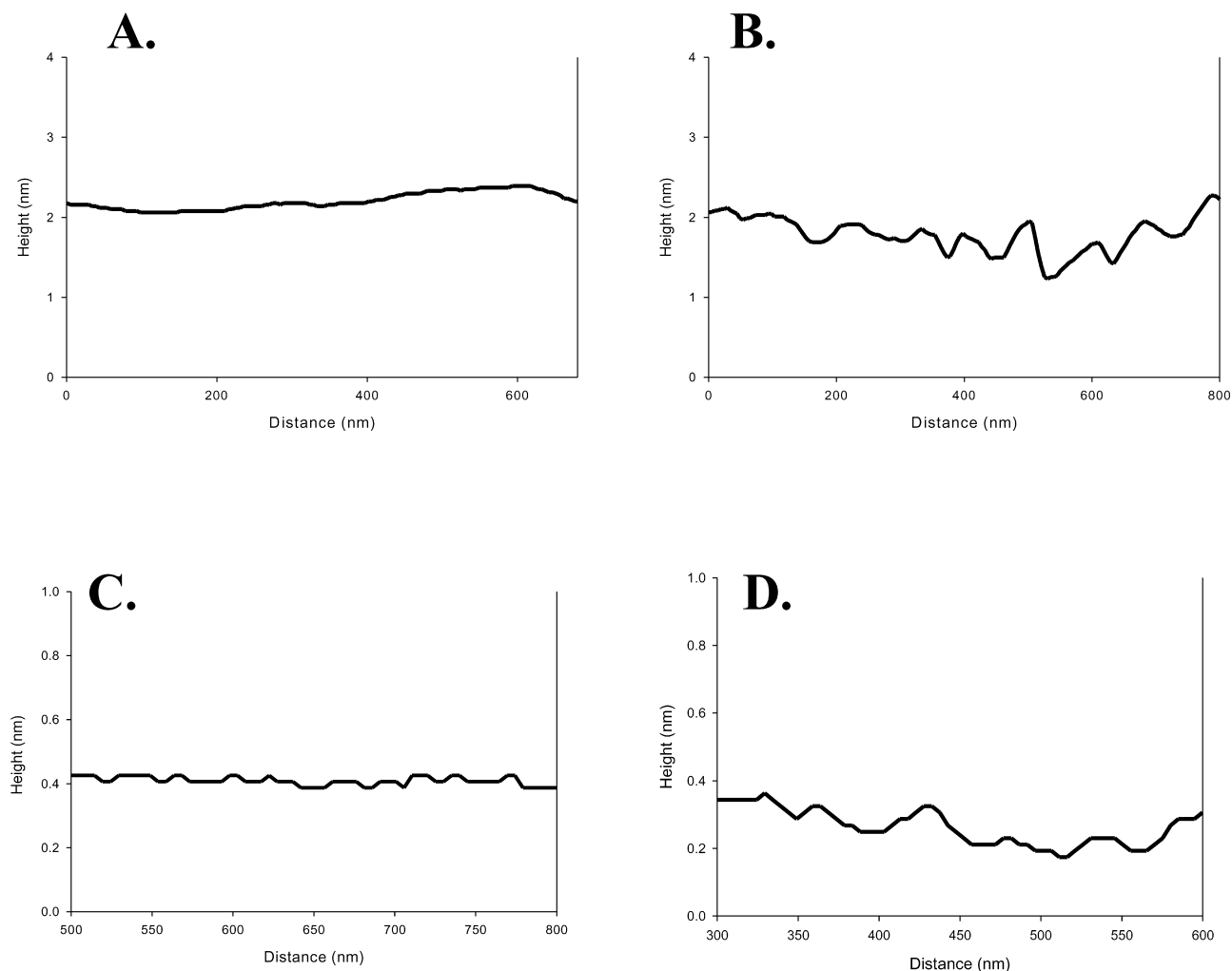


Fig. 5. A, Cross-section of PS continuous domain (imaged acquired in air). B, Cross-section of PS continuous domain (imaged acquired in water). C, Cross-section of PMMA discontinuous domain (image acquired in air). D, Cross-section of PMMA discontinuous domain (image acquired in water).

elastic factors is to compare friction image data collected when the probe is scanned from left to right and from right to left. If the contrast in the image reverses with scan direction, then tip adhesion and elastic effects cause the cantilever torsion; otherwise the signal is simply caused by sample topography. As seen in Fig. 6A,D that while the discontinuous domains can be distinguished in the friction image because of cantilever twisting at the domain edge, there is no significant difference between the magnitude of the friction signals between the domain interiors. This indicates that in air, differences in adhesive forces and elasticity between the two are inconsequential. Again, this is likely because of capillary forces that overwhelm the small differences in tip adhesion and polymer elasticity between domains. There is also no significant difference between images when the scan direction is reversed, indicating that the observed contrast is caused exclusively by sample topography. Ade et al. have carried out numerous investigations of immiscible PS/PMMA blend films made from low molecular weight polymers ($M_w \sim 27,000$) [14,15]. For these samples,

friction contrast between domains is observable in air; however, because of their low molecular weight, these samples anneal more quickly and completely, giving rise to stronger composition differentiation between domains. It is also worth noting that friction images collected in air are very susceptible to imaging artifacts. The most common artifact we encountered in these experiments is readily apparent in Fig. 6A, in which the contrast of the continuous domain suddenly jumps from a low value to a high value. While the exact reasons for these artifacts are unclear, no such effects were observed when imaging under water, suggesting they are related to perturbation of tip-sample forces by surface adsorbed water.

Considerably different results are obtained when friction imaging is carried out under water, as shown in Fig. 6C,D. The discontinuous domains show a clear contrast with the surrounding matrix and reversing the scan direction also reverses the contrast, indicating that sample topography does not play a significant role in this image. For the microscope detector geometry used here, the image in Fig. 6D reflects the 'true' friction signal—the bright, discontinuous

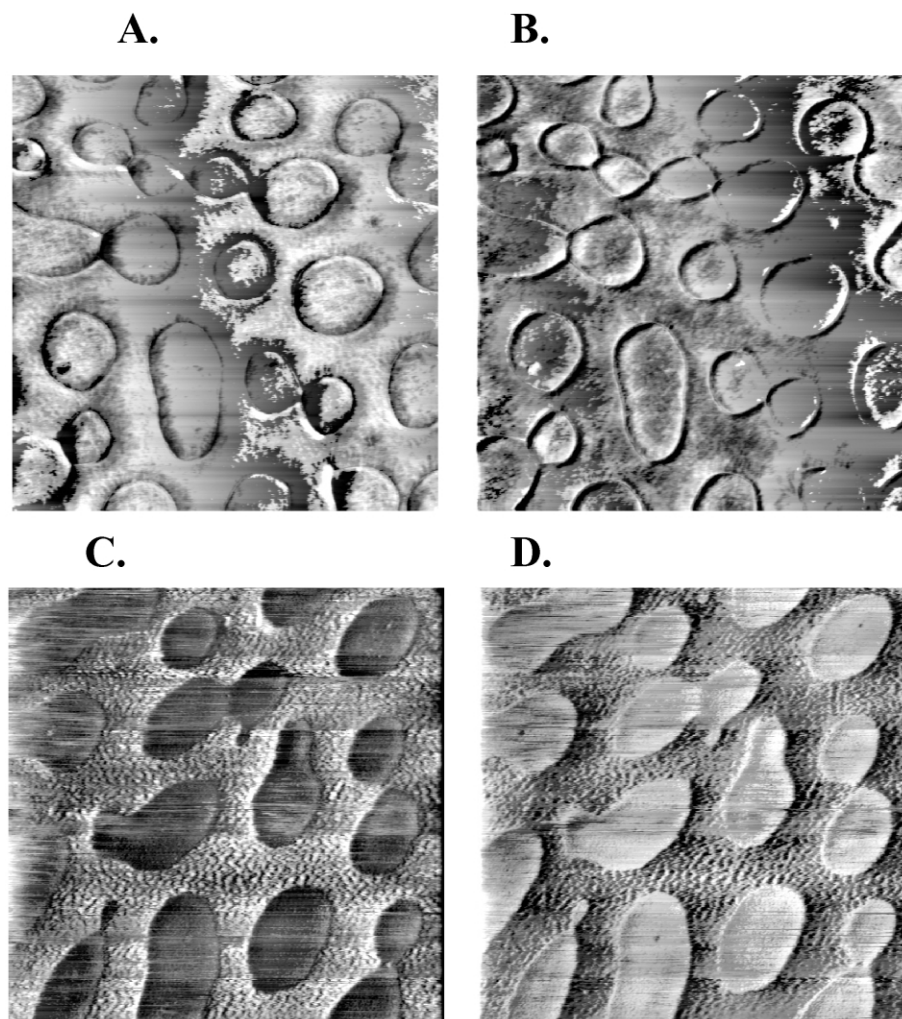


Fig. 6. A, B, Friction mode images ($5\ \mu\text{m} \times 5\ \mu\text{m}$) taken in air. Data was collected when the tip was scanned from right to left in (A) and from left to right (B). (C), (D), Friction mode image ($5\ \mu\text{m} \times 5\ \mu\text{m}$) taken in water. Data was collected when the tip was scanned from right to left in (C) and from left to right in (D).

domains correspond to greater torsion in the cantilever indicating that the probe–sample friction is larger than in the continuous domain. Higher friction in these domains reflects both the tip–sample adhesion and the elasticity of the sample [4]. Quantifying the tip–sample adhesion is problematic, because, as described above, we were unable to take force curve measurements of either domain without damaging the sample. However, as stated previously, Si_3N_4 AFM tips are slightly hydrophilic, and one might reasonably expect slightly higher adhesive forces with the PMMA-rich domains than with PS-rich domains. From the force curve measurements described previously, we also know that the sample softens substantially upon immersion in water. The second effect, a change in elasticity of the polymers, is likely the strongest contributor to the friction signal. One would expect the hydrophilic PMMA-rich to soften more significantly in water than the hydrophobic PS-rich domains. A softer sample will be more easily penetrated by the AFM tip, and a higher lateral force will be needed to move the tip through the sample. Magonov has illustrated

this effect and the importance of varying tip loading forces for determining relative polymer hardness in AFM by investigating friction force contrast behavior in micro-layered polyethylene samples [1]. For soft polymers, increasing loading forces should enhance friction contrast. Unfortunately, we had a very limited dynamic range of forces for our system, and could not substantially increase the loading force without inducing sample damage. As an alternative method for characterizing the elastic properties of this sample, and particularly any changes upon hydration, we have carried out phase imaging both in air and under water.

Intermittent contact mode images of the polymer film were taken in air, with topography and phase images collected simultaneously. There was no observable difference in film morphology between images taken in intermittent and contact mode, and the same region of the sample could be imaged repeatedly without damage. A typical phase image from this set of experiments, along with corresponding cross-sectional analysis, is shown in Fig. 7A,

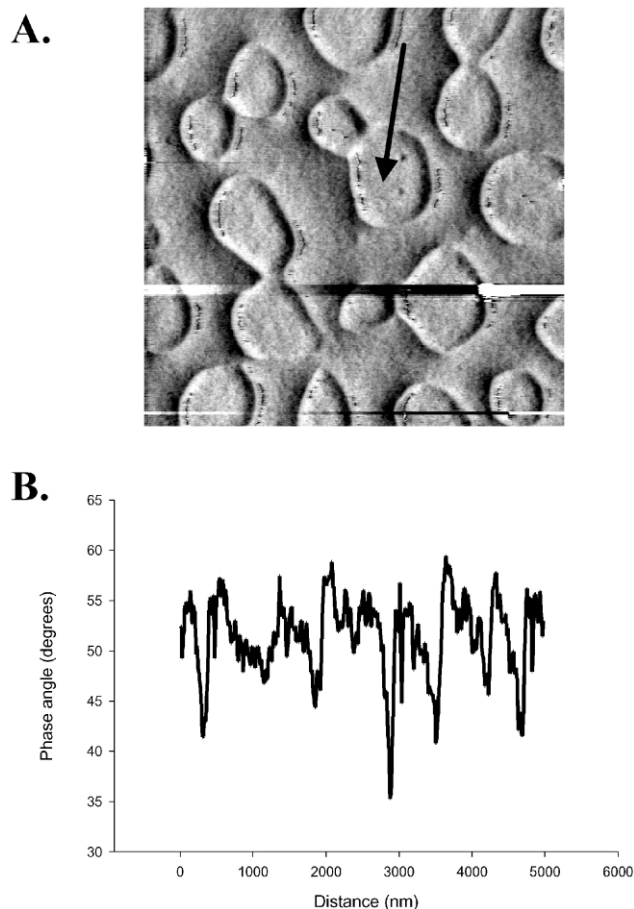


Fig. 7. A, Phase contrast image taken in air ($5\ \mu\text{m} \times 5\ \mu\text{m}$) at moderate tapping force. Note that while domain edges are highlighted, there is no difference in phase signal between the interior of the discontinuous domains (arrow) and the continuous domain. B, Cross-sectional analysis of phase contrast image in Fig. 7A.

D. As was the case with friction imaging in air, phase images highlighted the edges of the discontinuous domains but did not yield significant contrast between the interiors of the two different regions. Other than the valleys that correspond to the edges of the discontinuous domains, image cross-sections show no appreciable differences in phase signal levels. Because contrast in phase images can be strongly dependent on the magnitude of the tip–sample interaction force, we also examined the sample over a range of higher imaging forces. This failed to appreciably enhance contrast between the domain interiors. Under the ‘moderate force’ imaging regime (ratio of setpoint oscillation amplitude to free air amplitude of ~ 0.3 – 0.8), phase signals have been shown to yield information about surface stiffness related to local changes in Young’s modulus [12,16]. Specifically, high phase signals have been correlated with hard materials, which indicate that for the PS/PMMA blend sample in air, there is no significant difference in hardness between the two domains. This is in good agreement with the lack of contrast observed in the friction images collected in air; if the primary contributor to the friction signal were

elastic deformation, then one would not expect to see a difference in friction signal. Similarly, if preferential softening of the hydrophilic PMMA-rich domains were responsible for the friction contrast observed in water, one would expect the hard continuous domain to have a higher phase signal.

Phase images of the films under ultrapure water were collected, and a typical example, along with a corresponding cross-sectional analysis, is shown in Fig. 8A,B. Under these imaging conditions, there is now significant, measurable contrast between the interiors of the discontinuous domains and their surrounding matrix. The discontinuous domains had lower phase signals (typically ~ 6 – 7 degrees) than the continuous domains, indicating that the PMMA rich-domains are considerably softer than the PS-rich regions. These results are in excellent agreement with the model suggested by the friction images, which indicates that compositional contrast in this system is dominated by elastic effects from preferential softening of the PMMA-rich domains.

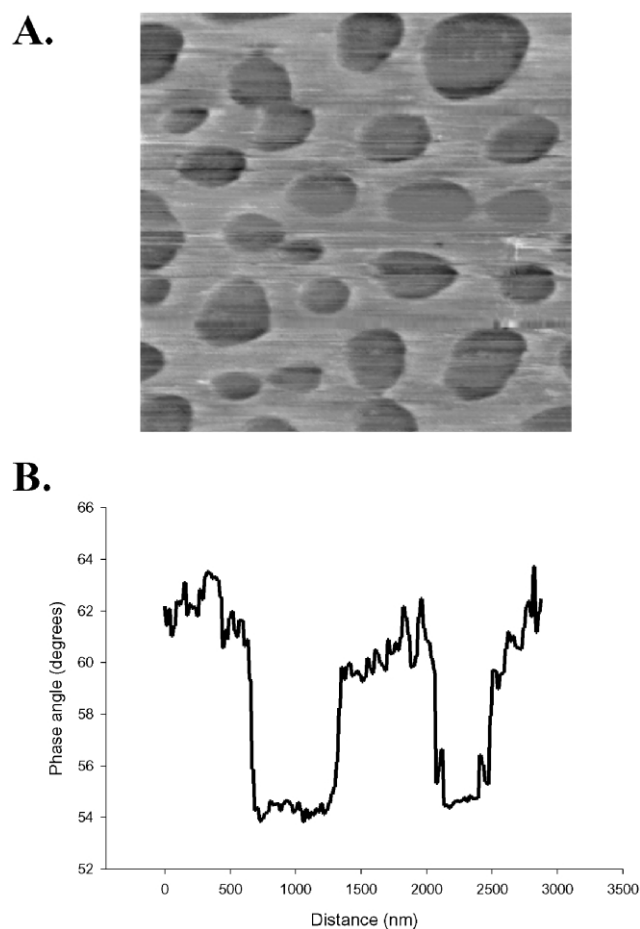


Fig. 8. A, Phase contrast image taken in water ($5\ \mu\text{m} \times 5\ \mu\text{m}$) at moderate tapping force. There is now a difference in phase signal between the discontinuous domain interiors and the surrounding continuous domain. B, Cross-sectional analysis of phase contrast image in Fig. 8A. The low-phase regions correspond to the discontinuous PMMA-rich domains, and the high-phase regions correspond to the continuous domain.

As is apparent from this study, dual use of friction force and phase imaging is a versatile, powerful approach for combined topographic and compositional mapping of polymer samples. It is worth noting that the samples investigated here provided a useful test case, but did not require us to operate the instrument at its limits in terms of sensitivity and spatial resolution. It should be possible to extend these measurements down to the nanometer length-scale, suggesting the possibility of resolving and chemically identifying nanoscale segregated domains and carrying out compositional mapping of polymers to the resolution of individual polymer molecules. Our future efforts in this area will be directed towards exploring the resolution limits of this combined imaging approach.

4. Summary

We have studied an immiscible PS/PMMA blend film using a combination of atomic force microscope imaging modes, including topographic, friction force and phase imaging. The polymer film segregates into discontinuous PMMA-rich domains, surrounded by a PS-rich continuous domain. In air, neither friction nor phase imaging provides contrast that is related to adhesive or elastic properties. However, both of these imaging techniques generate appreciable contrast when the sample is imaged in water. Contrast in both the friction and phase images is caused by a combination of tip-sample adhesion and elastic deformation of the sample. The latter effect is dominant for this sample, and we attribute the contrast observed in the images to preferential softening of the hydrophilic PMMA-rich domain over the PS-rich domain.

Acknowledgements

We thank Cynthia Morin and Adam Hitchcock from

McMaster University for providing samples, Stephen Urquhart from the University of Saskatchewan and Bob Reutter from Molecular Imaging Corporation for important contributions and discussion. This work was supported by the Natural Sciences and Engineering Research Council of Canada, the Saskatchewan Structural Sciences Centre and the University of Saskatchewan.

References

- [1] Magonov SN, Reneker DH. *Ann Rev Mater Sci* 1997;27:175–222.
- [2] Goh MC. Atomic force microscopy of polymer films. *Advances in chemical physics*, 91; 1995. p. 1–83.
- [3] Takano H, Kenseth JR, Wong SS, O'Brien JC, Porter MD. *Chem Rev* 1999;99:2845–90.
- [4] Ross M, Steinem C, Galla HJ, Janshoff A. *Langmuir* 2001;17:2437–45.
- [5] Schneider J, Dufrene YF, Barger Jr. WR, Lee GU. *Biophys J* 2000;79:1107–18.
- [6] Overney RM, Meyer E, Frommer J, Guntherodt HJ, Fujihira M, Takano H, Gotoh Y. *Langmuir* 1994;10:1281–6.
- [7] Noy A, Frisbie CD, Rozsnyai LF, Wrighton MS, Lieber CM. *J Am Chem Soc* 1995;117:7943–51.
- [8] Noy A, Vezenov DV, Lieber CM. *Ann Rev Mater Sci* 1997;27:381–421.
- [9] Noy A, Sanders CH, Vezenov DV, Wong SS, Lieber CM. *Langmuir* 1998;14:1508–11.
- [10] Hansma HG, Kim KJ, Laney DE, Garcia RA, Argaman M, Allen MJ, Parsons SM. *J Struct Biol* 1997;119:99–108.
- [11] Prater CB, Maivald PG, Kjoller KJ, Heaton MG. Digital instruments application note: TappingMode imaging applications and technology. Santa Barbara: Digital Instruments; 2003.
- [12] Magonov SN, Elings V, Whangbo MH. *Surf Sci* 1997;375:L385–91.
- [13] Morin C, Ikeura-Sekiguchi H, Tyliczszak T, Cornelius R, Brash JL, Hitchcock AP, Scholl A, Nolting F, Appel G, Winesett DA, Kaznacheyev K, Ade H. *J Electron Spectrosc Relat Phenom* 2001;121:203–24.
- [14] Ade H, Winesett DA, Smith AP, Qu S, Ge S, Sokolov J, Rafailovich M. *Europhys Lett* 1999;45:526–32.
- [15] Winesett DA, Ade H, Sokolov J, Rafailovich M, Zhu S. *Polym Int* 2000;49:458–62.
- [16] McLean RS, Sauer BB. *Macromolecules* 1997;30:8314–7.